IMA Journal of Applied Mathematics (2000) **65**, 147–171

On the unsteady motion of two-dimensional sails

A. D. FITT
Faculty of Mathematical Studies, University of Southampton, Southampton SO17 1BJ*, UK*

AND

T. R. B. LATTIMER
OCIAM, Mathematical Institute, 24–29 *St Giles, Oxford* OX1 3LB*, UK*

[Received 12 November 1998]

An equation is derived to describe the motion of a two-dimensional inextensible sail at a small, time-dependent, angle of incidence to a uniform two-dimensional flow. The equation derived is a singular partial integro-differential equation, which in the steady case reduces to the sail equation of Voelz. A number of limiting versions of the equation are derived and analysed for cases where the relative mass of the sail is large or small. For general unsteady sail motions the governing equation must be solved numerically. A scheme is proposed that employs Chebyshev polynomials to approximate the position of the sail; ordinary differential equations are derived to determine the relevant Chebyshev coefficients and a number of examples are illustrated and discussed. It is found that in some cases where the angle of attack changes sign the tension may become large; in these instances the underlying physical assumptions of the model may be violated.

1. Introduction

The study of flow past a flexible membrane has been of interest for many years, with the obvious application to flow past a sail. To date most studies of flow past a sail have been two-dimensional. One of the first mathematical models was proposed by Cisotti (1932). In this study the sail was assumed to be non-porous, with the flow separating at the trailing edge of the sail (the 'leach'), to form a quiescent wake. This differed from the work of Voelz (1950), in whose model the sail was considered as a distribution of vortices, the flow being considered to be incompressible and irrotational, and the sail assumed to be non-porous and inextensible. It is this model upon which the analysis in this study will largely be based. Voelz's model applied thin aerofoil theory (see, for example, Van Dyke (1964)), assuming that the sail deviates from a straight line connecting the masts by only a small amount, thus permitting linear asymptotic analysis to be used, subject to the assumption that the angle of attack of the cross-flow remains small. By this means a linear integro-differential equation (depending on the ratio of the angle of attack to the excess length of the sail) was derived for the shape of the sail. This equation was then solved numerically for a variety of sail lengths, and the lift, moment, and pressure distribution on the sail were also calculated. Bugler (1957) undertook a more thorough analysis based on a similar model. However it is the work of Thwaites (1961) that is most usually associated with this problem. Thwaites's work was similar to that of Voelz, but although Thwaites

(independently) derived the same equation of motion, his work extended the theory to apply to a porous sail where the flow through the sail was proportional to the pressure difference across it. Moreover Thwaites found solutions beyond the range examined by Voelz, in particular finding a range of solutions with zero lift for a non-zero angle of attack. Nielsen (1963) independently completed a study similar to that of Thwaites based on Fourier series and numerical matrix techniques rather than integral equations, and found that his results were in good agreement with those of Thwaites and Voelz. Nielsen also examined the three-dimensional problem, and performed some experiments. The experiments largely agreed with the numerical calculations, with errors thought to be caused in part by porosity of the sail and boundary-layer effects, although Chapleo (1968) argued that errors may have been caused by overestimation of the lift due to camber. Barakat (1968) studied the influence of the porosity of the sail and extended the theory to a two-lobed sail, and Tuck & Haselgrove (1972) considered the problem in which the sail is not rigidly attached to the trailing edge but instead attached to a rope, or sheet, which is inflexible and fixed at one end. They found that as the length of the sheet increases the lift decreases but the stability of the sail increases. A three-dimensional linear analysis was completed by Nickel (1987), using the 'lifting line theory' of Prandtl (1918).

A more general study, valid for larger angles of incidence than those considered by Voelz or Thwaites was completed by Dugan (1970) who used the behavioural model developed by Cisotti. This was a nonlinear free-streamline model, allowing separation of the flow at the trailing edge, assuming constant tension in the sail. A nonlinear singular integral equation was found and solved numerically, thus obtaining the sail profile and the drag, lift and moment experienced by the sail, although the model breaks down for small angles of attack. Vanden-Broeck (1982) used a similar model to derive and numerically solve an integro-differential equation for arbitrary angles of incidence. Jackson (1983) considered an extensible sail, and derived a nonlinear equation for arbitrary angles of attack. Computational procedures were also used for a viscous flow with a Reynolds number of between 2×10^3 and 10^4 for elastic, inextensible, and constant tension sails, by Smith & Shyy (1995a) for steady flow, and Smith & Shyy (1995b) for unsteady flow. Other unsteady analyses include that of Bäcker *et al.* (1991), for the related nonlinear problem of fibres fluttering in an air spinning process, and that of Haselgrove & Tuck (1976), who studied a finite-length sail whose rear end was connected to the downstream mast by a length of 'two-dimensional sheeting'. They investigated small disturbances from steady sail profiles, finding that there was a critical value of the sail tension which, if not attained, led to instability. In some respects their model was similar to the one presented below, though they did not study general unsteady sail motions. There are, however, major differences. The fact that Haselgrove & Tuck considered a massless sail meant that sail inertia was not important. As we shall see below, this effect can dominate the flow under some circumstances. Another key difference between their model and ours is the inclusion in the former of an infinite wake downstream of the sheeting. Once again, this materially alters the results.

Although the models of Voelz, Thwaites, and Nielsen, and the equations derived, are essentially the same, comparisons to the steady results will be made using the work of Thwaites (1961) (henceforth referred to as 'Thwaites'), as this is the most complete and detailed analysis of the theoretical steady problem. A key finding of Thwaites is the non-uniqueness of the sail shape for sufficiently small angles of attack. For all non-zero angles

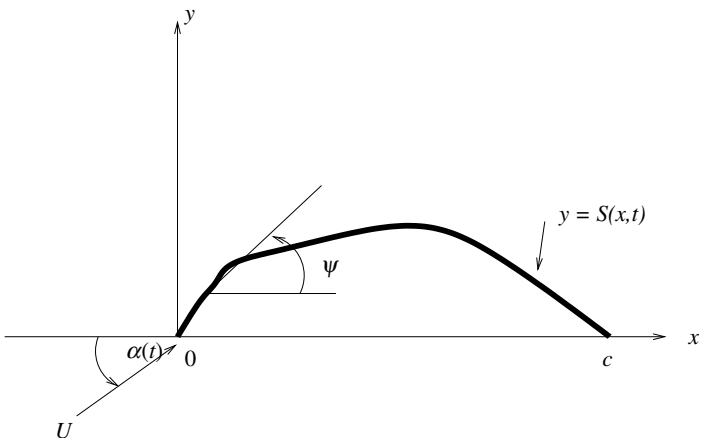

FIG. 1. Schematic diagram of sail geometry.

of attack exactly one concave solution with the sail shape the same sign as the angle of attack exists, but for smaller angles of attack there are a finite number of other solutions, corresponding to lower values of the tension, with each lower tension positive and negative solution pair containing one more inflexion than the previous one.

2. Equation of motion

The majority of previous studies (in particular Thwaites (1961) and Voelz (1950)) have considered the flow of a uniform stream at a constant angle of incidence α to a two-dimensional, inextensible, porous sail. The goal of this study is to consider the case where the angle of attack α is a function of time, so that the sail shape $y = S(x, t)$ is also time-dependent. This case is clearly of greater practical value than the purely steady case, and has not been examined previously for a sail of non-zero mass. For simplicity the porosity of the sail will henceforth be taken to be zero, although the extensions required to the analysis below to include the effects of porosity are not difficult. A schematic diagram of the flow is shown in Fig. 1.

For consistency we largely follow Thwaites's notation. We assume the length of the sail to be given by $c(1+\epsilon)$, where c is the distance between the masts. This defines ϵ, the small parameter in the problem. (Other definitions are possible; Thwaites based his scalings on the small parameter α, but since in this case α is time-dependent, this is a less convenient variable to use.) The sail shape thus satisfies

$$c(1+\epsilon) = \int_0^c (1 + S'^2(x))^{\frac{1}{2}}\, \mathrm{d}x, \tag{1}$$

which implies that $S = O(c\sqrt{\epsilon})$. Ultimately, (1) will be used to close the model and determine the sail shape for a given excess length and angle of attack.

Under the assumptions of incompressible, irrotational, inviscid flow, the velocity

potential Φ for the flow is given by

$$\Phi(x, y, t) = U(x\cos\alpha(t) + y\sin\alpha(t)) + \frac{1}{2\pi}\int_0^c \gamma(\xi, t)\arctan\left(\frac{y}{\xi - x}\right)\mathrm{d}\xi, \qquad (2)$$

where γ is the (unknown) vortex strength at a given point on the sail. We assume that γ is small compared to U (in a sense that will be quantified later) so that the sail constitutes only a small perturbation to uniform flow. The condition that the sail is a free boundary is

$$\frac{D}{Dt}(y - S(x, t)) = 0,$$

which gives

$$\frac{\Phi_y}{\Phi_x} = S_x + \frac{S_t}{\Phi_x}. \qquad (3)$$

The derivatives of Φ on the sail may be obtained from (2) by taking the limit as $y \to 0$, yielding (for $\alpha \ll 1$)

$$\Phi_x = U(1 + O(\alpha^2)) + O(\gamma),$$
$$\Phi_y = U\alpha + \frac{1}{2\pi}\int_0^c \frac{\gamma(\xi, t)}{\xi - x}\,\mathrm{d}\xi + o(\alpha).$$

Since $S = O(c\sqrt{\epsilon})$, this (along with (3)) immediately shows that $\gamma = O(U\alpha)$, and that $\alpha = O(\epsilon^{\frac{1}{2}})$. To leading order therefore

$$S_x + \frac{S_t}{U} = \alpha(t) + \frac{1}{2\pi U}\int_0^c \frac{\gamma(\xi, t)}{\xi - x}\,\mathrm{d}\xi. \qquad (4)$$

Equation (4) relates the vortex distribution γ to the sail shape S. To further relate γ to S, we perform a force balance on a sail element. It is convenient to express the vertical force per unit area of sail exerted on the sail as the sum of the force per unit area F_T resulting from the tension in the sail, and the aerodynamic force per unit area, F_A. The equation governing the motion of the sail over an element of the sail with arc length δs is then

$$F_T\delta s + F_A\delta s = \rho'\delta s\frac{\partial^2 S}{\partial t^2}, \qquad (5)$$

where ρ' is the mass per unit area of the sail (kg/m^2).

To determine F_T, consider an element of the sail of length δs whose tangent makes an angle ψ with the x-axis and whose end-points are at $(x, S(x))$ and $(x + \delta x, S(x + \delta x))$ respectively. Comparison of forces in the x-direction shows that $\delta T = 0$ to lowest order, where T is the tension force per unit area of the sail. The y-component F_T is therefore given by

$$F_T = (T + \delta T)\sin(\psi + \delta\psi) - T\sin\psi \simeq T\cos\psi\delta\psi. \qquad (6)$$

The aerodynamic force per unit area, F_A, satisfies

$$F_A\delta s = (p^- - p^+)\delta s\cos\psi$$

and to leading order is therefore simply the pressure difference across the sail at a given point. It may therefore (in the absence of body forces, which could easily be included if desired) be determined from Bernoulli's equation in the form

$$\lim_{y\to 0^+}\left(\Phi_t + \frac{p}{\rho} + \tfrac{1}{2}\boldsymbol{q}^2\right) = \lim_{y\to 0^-}\left(\Phi_t + \frac{p}{\rho} + \tfrac{1}{2}\boldsymbol{q}^2\right), \tag{7}$$

where ρ is the density of the free stream (kg/m^3) and the fluid velocity is denoted by $\boldsymbol{q}$. This may be written in the form

$$[\Phi_t]_{0^-}^{0^+} + \left[\frac{p}{\rho}\right]_{0^-}^{0^+} + \tfrac{1}{2}\left[\boldsymbol{q}^2\right]_{0^-}^{0^+} = 0. \tag{8}$$

It is easiest to consider the three terms separately. Equation (2) gives

$$\Phi_t = U\alpha'(t)(y\cos\alpha(t) - x\sin\alpha(t)) + \frac{1}{2\pi}\int_0^c \gamma_t(\xi, t)\arctan\left(\frac{y}{\xi - x}\right)\mathrm{d}\xi. \tag{9}$$

The first term in this equation is clearly continuous across the boundary $y = 0$. The integrand in the second term is also continuous in y, except possibly at $\xi = x$. However, this part of the integral does not contribute to (8) since at this point we make the standard assumption, common to many studies of this form, that the motion of the sail is not affected by the vorticity that it sheds.

The pressure term in (8) is simply $[p/\rho]_{0^-}^{0^+}$ which is $-F_A$. The third term is $\rho U\gamma(x, t)$ as in the steady case. Thus (8) becomes

$$F_A = \rho U\gamma(x, t). \tag{10}$$

We may combine (5), (6) and (10) to give

$$\rho' S_{tt}\delta s = T\cos\psi\,\delta\psi + \rho U\gamma\cos\psi\,\delta s + O(\psi\delta\psi),$$

and hence, in the limit as ψ tends to zero,

$$\rho U\gamma(x, t) + TS_{xx} = \rho' S_{tt}. \tag{11}$$

This gives an expression for γ which may in turn be substituted into (4) to give the *time-dependent sail equation*,

$$S_x + \frac{S_t}{U} = \alpha(t) + \frac{1}{2\pi\rho U^2}\int_0^c \frac{\rho' S_{tt}(\xi, t) - TS_{\xi\xi}(\xi, t)}{\xi - x}\,\mathrm{d}\xi. \tag{12}$$

The boundary conditions merit some discussion. Since the two ends of the sail are fixed, we have $S(0, t) = S(c, t) = 0$. The system may be closed by invoking the Kutta condition, which asserts that the fluid velocity at the trailing edge of the sail is finite. Examining the expressions for Φ_x and Φ_y, we see that this requirement is tantamount to assuming that both γ and

$$\int_0^c \frac{\gamma(\xi, t)}{\xi - x}\,\mathrm{d}\xi$$

are bounded at $x = c$. The latter can only occur if $\gamma - A(t)(c-x)^{-1/2} \to 0$ for some $A(t)$; the former then requires that $A(t)$ must be zero, and thus γ itself must be zero at the sail trailing edge. Equation (11) now requires that $S_{xx}(c, t)$ must be zero if the Kutta condition is to be satisfied, a result identical to that which applies for the steady equation.

The unsteady equation may also be expressed in non-dimensional coordinates; we set

$$x = cx^*, \qquad \xi = c\xi^*, \qquad t = \frac{c}{U}t^*, \qquad S(x, t) = c\epsilon^{\frac{1}{2}}S^*(x^*, t^*),$$

$$\mu = \frac{2\rho c}{\rho'}, \qquad \beta = \left(\frac{T}{\rho' U^2}\right)^{\frac{1}{2}}, \qquad \alpha(t) = \epsilon^{\frac{1}{2}}\alpha^*(t^*).$$

In these coordinates (12) becomes

$$\frac{1}{\pi}\int_0^1 \frac{S^*_{t^*t^*} - \beta^2 S^*_{\xi^*\xi^*}}{\xi^* - x^*}\,\mathrm{d}\xi^* = \mu(S^*_{x^*} + S^*_{t^*} - \alpha^*(t^*)), \tag{13}$$

with the boundary conditions $S^*(1, t^*) = S^*(0, t^*) = 0$ and $S^*_{x^*x^*}(1, t^*) = 0$. The initial conditions necessary are that the values of S^* and $S^*_{t^*}$ are specified for $x^* \in [0, 1]$. As expected, when all time derivatives are set to zero, the steady sail equation of Voelz (1950) is recovered. The equation (13) is dependent on the two non-dimensional parameters μ and β. Of these, μ is dependent only upon the initial conditions and is constant in space and time. Whilst at any particular instant in time the tension T is also constant to leading order (a consequence of the force balance in the x-direction), it must be chosen so that the solution of (13), $S(x, t)$, has constant length. The tension (and hence the quantity β) must therefore be regarded as being an unknown function of time. In addition to the equation of motion and the boundary and initial conditions, the length condition (1) must be satisfied. With the above scalings, the length condition becomes

$$1 = \tfrac{1}{2}\int_0^1 S^{*\prime 2}(x^*, t^*)\,\mathrm{d}x^* + O(\epsilon). \tag{14}$$

A solution for $S^*(x^*, t^*)$ for a given β will therefore not be regarded as a physical solution (that is, a solution which conserves sail length) unless that solution satisfies (14) *for all values of* t^*. This may not be possible for constant values of β and so the tension, β, must be considered as a function of time.

The net lift on the sail is an important variable to determine. The force on each mast may be calculated by considering an element of length δx at the end of the sail. Since in this linear model all forces are horizontal to leading order and the tension, T, is constant, the horizontal force on each mast has magnitude T, that is, $2\rho U^2 c\beta^2/\mu$. In the y-direction the force on the mast is given by the y-component of the tension, namely $T\psi$, and thus (in non-dimensionalized coordinates) the force on the upstream mast is $2\rho U^2 c\epsilon^{\frac{1}{2}}\beta^2 S^{*\prime}(0)/\mu$, whilst the force on the downstream mast is $-2\rho U^2 c\epsilon^{\frac{1}{2}}\beta^2 S^{*\prime}(1)/\mu$. The net lift on the sail is thus

$$L(t) = \frac{2\beta^2\rho U^2 c}{\mu}\epsilon^{\frac{1}{2}}(S^*_{x^*}(0, t) - S^*_{x^*}(1, t)). \tag{15}$$

From a practical point of view, (15) is particularly easy to work with as it involves only the derivatives of the sail shape at $x^* = 0$ and $x^* = 1$.

3. Steady solutions to the sail equation

With α^* constant and all time derivatives set equal to zero, (13) becomes the extensively studied non-dimensional steady sail equation

$$-\frac{1}{\pi}\int_0^1 \frac{S^*_{\xi^*\xi^*}}{\xi^* - x^*}\,\mathrm{d}\xi^* = \lambda(S^*(x^*) - \alpha^*), \tag{16}$$

with

$$S^*(0) = S^*(1) = S^{*\prime\prime}(1) = 0, \qquad 1 = \tfrac{1}{2}\int_0^1 S^{*\prime 2}\,\mathrm{d}x^*,$$

where, for consistency with previous authors, we have set $\lambda = \mu/\beta^2$. Since we shall frequently use solutions to (16) as initial conditions for unsteady calculations we briefly review the more important properties of (16).

Although no closed-form solutions of (16) are known, many different numerical methods have been proposed and successfully used to solve (16). (When steady calculations were required in this study, we used a Chebyshev collocation method.) Assuming that the linear singular integro-differential equation (16) possesses a unique solution for specified values of α^* and λ subject to the boundary conditions $S^*(0) = S^*(1) = S^{*\prime\prime}(1) = 0$, values of λ (and thus of the sail tension) may be inferred for a given angle of attack α^* by choosing λ so that the length condition is satisfied. Figure 2 shows λ plotted against α^*, and suggests that it is simpler to regard λ as specified and α^* as calculated. The fact that the (α^*, λ) curve shown in Fig. 2 is not one-to-one when $\alpha^* < \alpha_c^* \sim 0{\cdot}971$ is of interest. For a fixed value of α^* less than α_c^* the lowest possible value of λ in Fig. 2 corresponds to a concave sail shape where S^* has the same sign as α^*, much as one might expect. As λ increases, the next branch of the curve gives solutions where $S^{*\prime\prime}$ is still of one sign, but S^* and α^* are of opposite signs. Branches further up the diagram correspond to sail shapes that cross the axis an increasing number of times. Few attempts have been made to determine the stability of these multiple solutions (though see Haselgrove & Tuck (1976)). One reason for studying the unsteady version of the problem is to try to determine whether or not any of the more highly oscillatory sail shapes are stable and might ever be expected to be observed.

Another property of interest in the steady case is the lift, which is given by (15). For certain values of λ, the flow satisfies a Kutta condition at $x^* = 0$ as well as at $x^* = 1$. The first six such eigenvalues are given by $\lambda = 2{\cdot}316, 5{\cdot}507, 8{\cdot}635, 11{\cdot}78, 14{\cdot}93$ and $18{\cdot}08$; asymptotic formulae may be developed for larger eigenvalues. Solutions corresponding to even-numbered eigenvalues are antisymmetric about $x^* = \frac{1}{2}$ and have zero lift, whilst odd-numbered eigenvalues are symmetric about $x^* = \frac{1}{2}$ and also generate solutions for the case $\alpha^* = 0$.

4. Limiting cases of the sail equation

The unsteady sail equation (13) is a partial singular integro-differential equation. Moreover, because of the need to determine $\beta(t)$ such that (14) is satisfied, it is nonlinear. In general, therefore, it will be necessary to determine solutions numerically. Parametrically, (13)

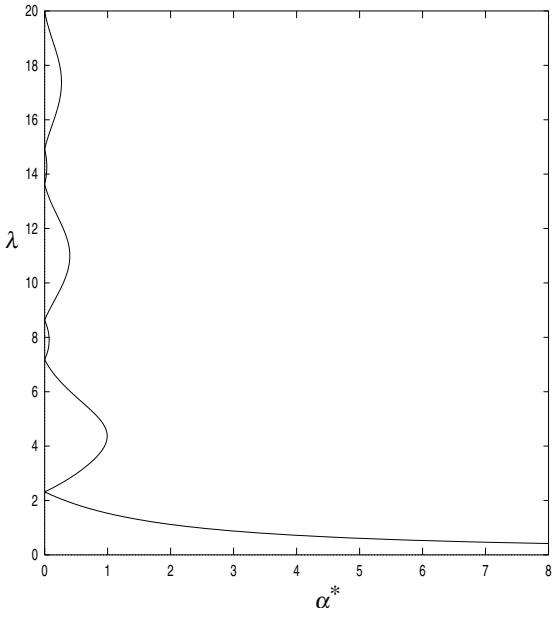

FIG. 2. Calculated values of λ vs. α^* for steady sail equation.

depends upon the scaled angle of incidence α^*, the tension β, and μ, an inverse measure of the mass of the sail. Of these the value of β is determined by the length condition, so that for a sail of a given length the shape depends only upon α^* and μ. Clearly both large and small values of α^* are of interest, and although a typical sail in air would have to be very long before μ became large, for flexible sheets in water or other liquids μ may well be large. Thus both large and small values of μ are also of interest. Before embarking on a full numerical solution of the problem, we examine various limiting forms of the equations that correspond to large and small values of α^* and μ. As well as giving rise to some interesting mathematical problems and conclusions in themselves, these limiting cases may, under some circumstances, be used to provide validation for numerical methods.

Two limiting cases may be dealt with immediately: when $\alpha^* \ll 1$, we simply obtain one of the steady solutions corresponding to $\alpha^* = 0$. When $\mathrm{d}\alpha^*/\mathrm{d}t^* \ll 1$ the angle of incidence changes too slowly for fully unsteady effects to be important, the problem is quasi-steady and solutions may be calculated by merely solving a sequence of steady problems parametrized by t^*.

4.1 *Small mass limit*

Consider first the case where the mass of the sail is small so that $\mu \gg 1$. Dividing (13) by μ gives

$$\frac{1}{\mu\pi}\int_0^1 \frac{S^*_{t^*t^*} - \beta^2 S^*_{\xi^*\xi^*}}{\xi^* - x^*}\,\mathrm{d}\xi^* = S^*_{x^*} + S^*_{t^*} - \alpha^*(t^*) \tag{17}$$

and, assuming that both β and α^* remain of order 1, suggests that the correct leading-order equation is

$$S^*_{x^*} + S^*_{t^*} - \alpha^*(t^*) = 0.$$

This equation has the general solution

$$S^* = f(x^* - t^*) + A(t^*),$$

where f is an arbitrary function and $A_{t^*} = \alpha^*$. We must now consider the boundary conditions. Clearly if it is to be true that $S^*(0) = S^*(1) = 0$ then necessarily

$$f(1 - t^*) + A(t^*) = 0 \quad \text{and} \quad A(t^* - 1) \equiv A(t^*), \tag{18}$$

which rules out a solution for general $\alpha^*(t^*)$. Nevertheless for periodic functions α^* with period 1, solutions may exist. We interpret such solutions as oscillatory eigenvalue solutions where both the lift and the tension are small relative to $\rho U^2 c$; specifically the sail tension is $O(\rho' U^2)$ and the lift is $O(\rho' U^2 \sqrt{\epsilon})$. A further restriction is placed on α^* by the length condition, which requires that

$$\tfrac{1}{2} \int_1^{1+r} \alpha^{*2}(q)\, \mathrm{d}q = 1$$

for arbitrary r. For example, if $\alpha^* = 2 \cos 2n\pi t^*$, then the function

$$S^*(x^*, t^*) = \frac{1}{n\pi} \left(\sin 2n\pi (x^* - t^*) + \sin 2n\pi t^* \right) \tag{19}$$

is a solution that satisfies the length condition for all integer values of n. Although (19) has the property that $S^*(0, t^*) = S^*(1, t^*) = 0$, the Kutta condition does not hold. As might be anticipated, however, after further investigation it transpires that the problem is of singular perturbation type, and in a boundary layer of width $O(1/\mu)$ near $x^* = 1$ an inner problem applies where time derivatives are negligible. Here the problem becomes quasi-steady and the Kutta condition is satisfied. In this region, the length condition is not affected to leading order.

Figure 3 shows a plot of (19) for $n = 1$, with t^* taking the values 0, 0·2, 0·4, 0·6, 0·8. The solution is periodic with period 1.

For functions α^* that do not satisfy (18), or are not periodic with period 1, a solution for $\mu \ll 1$ is clearly not possible with the above assumptions. This is because the assumption that β remains of order 1 is dangerously naive, particularly bearing in mind the dependence of the tension on the angle of incidence in the steady-state problem. In general, we find that for large values of μ the correct asymptotic balance is achieved by assuming that β^2 scales with μ. Thus only the $S^*_{t^*t^*}$ term is negligible in (17) and the leading-order equation becomes

$$-\frac{1}{\pi} \frac{\beta^2}{\mu} \fint_0^1 \frac{S^*_{\xi^*\xi^*}}{\xi^* - x^*}\, \mathrm{d}\xi^* = S^*_{x^*} + S^*_{t^*} - \alpha^*(t^*) + O(\mu^{-1}), \tag{20}$$

with the same boundary conditions as before, save for the fact that only S^* rather than S^* and $S^*_{t^*}$ must be prescribed at $t^* = 0$. (For $t^* \ll 1$ a small-t^* boundary layer must be

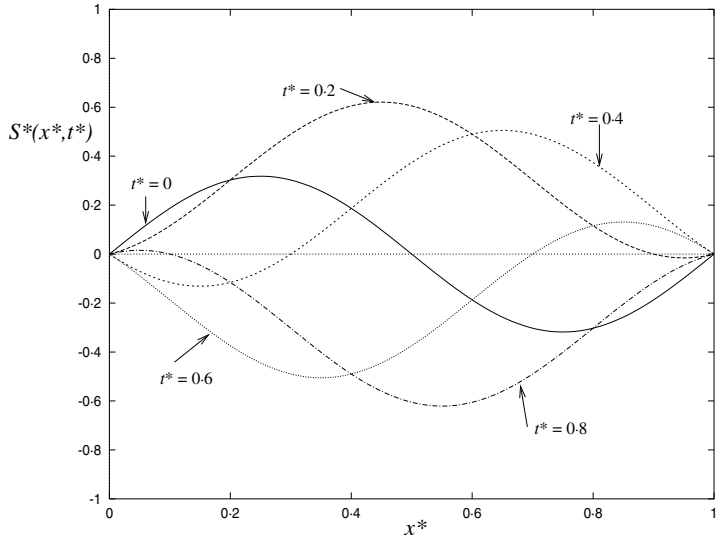

FIG. 3. Successive sail shapes for a small mass sail with $O(1)$ tension.

taken into account; we do not pursue this further here.) A numerical scheme to solve this equation is described in Lattimer (1996).

The above analysis has assumed that α^* remains of order 1. For a sail of low mass with a high angle of incidence (that is, $\mu \gg 1$ and $\alpha^* \gg 1$) the α^* term dominates the right-hand side of (20), requiring that $\beta^2 = O(\mu\alpha^*)$ and giving essentially the same equation as for the steady-state case for large α^*, namely

$$\frac{1}{\pi}\frac{\beta^2}{\mu}\int_0^1 \frac{S^*_{\xi^*\xi^*}}{\xi^* - x^*}\,\mathrm{d}\xi^* = \alpha^*(t^*) + O(\mu^{-1}) + O(\alpha^{*-1}).$$

This has the same solution as the steady-state equation for large λ given by Thwaites (1961).

4.2 *The solution for large α^**

Although α must be much less than one to satisfy the assumption that the deflection from the uniform stream is small, there is no reason why α^* (defined by $\alpha\epsilon^{-\frac{1}{2}}$) should remain of order 1. The behaviour for large α^* when μ is large or small has been discussed at the end of the two preceding sections. If μ is of order 1 then in order for (13) to balance, β^2 must scale with α^*, and all other terms are negligible, leaving

$$\frac{1}{\pi}\int_0^1 \frac{S^*_{\xi^*\xi^*}}{\xi^* - x^*}\,\mathrm{d}\xi^* = \mu\frac{\alpha^*}{\beta^2}. \tag{21}$$

In this case solutions are therefore quasi-steady, similar to those discussed by Thwaites (1961) for a high tension (or, equivalently, high angle of incidence) sail. We note also that

the solution of (21) clearly scales with $\mu\alpha^*\beta^{-2}$ which, according to the length condition, must be constant. Thus β^2 is proportional to α^* and S^* is completely independent of time. Equation (21) may now be solved by standard methods to yield

$$\beta^2(t^*) = \mu\alpha(t^*)\sqrt{\frac{3\pi^2}{128} - \frac{1}{6}}.$$

Physically, this result may be interpreted as stating that a high relative angle of incidence implies a high tension. The inertia of the sail becomes negligible relative to the forces acting upon it and the equation of motion becomes a balance between the tension and the uniform part of the flow. Since only one sail shape provides the right balance for this, this shape remains constant so long as α^* is much greater than unity, even though α^* might vary with time.

4.3 *Large mass limit*

For a sail of large mass per unit area, the parameter μ may be taken to be asymptotically small. For order 1 values of α^* in the limit as $\mu \to 0$, the right-hand side of (13) tends to zero and thus the finite Hilbert transform of $S^*_{t^*t^*} - \beta^2 S^*_{x^*x^*}$ must be zero, so $S^*_{t^*t^*} - \beta^2 S^*_{x^*x^*}$ must be proportional to $x^{*-\frac{1}{2}}(1 - x^*)^{-\frac{1}{2}}$. The Kutta condition $S_{x^*x^*} = 0$ may now be applied to show that, when α^* is of order 1,

$$S^*_{t^*t^*} - \beta^2 S^*_{x^*x^*} = 0, \tag{22}$$

with the usual boundary conditions and the length condition applying. The initial conditions for (22) determine the evolution of β; if $S^*_{t^*} = 0$ initially and $S^*(x^*, 0) = S^*_0(x^*)$ then $\beta = 0$ and $S^*(x^*, t^*) \equiv S^*_0(x^*)$, a physically reasonable conclusion which simply asserts that the sail is too heavy to be moved by a free stream of small angle. If $S^*_{t^*}$ is initially non-zero then the sail has inertia and in general β is an order 1 function of time. Although in this case the aerodynamic effects are negligible, the inertia effects are balanced by the tension to leading order. The governing equation is a wave equation with a non-constant wave speed, reflecting the requirement that the tension varies in such a way as to preserve the sail length. The sail therefore behaves like a string under variable tension, with the length being fixed not only at leading order, but also at the level defined by the perturbations of the string.

If α^* is of order μ^{-1}, then the free stream is able to influence the sail motion and the final term in (13) is significant. The sail shape now satisfies the partial singular integro-differential equation

$$\frac{1}{\pi}\int_0^1 \frac{S^*_{t^*t^*} - \beta^2 S^*_{\xi^*\xi^*}}{\xi^* - x^*}\,\mathrm{d}\xi^* = -\mu\alpha^*(t). \tag{23}$$

When (23) is inverted using standard methods detailed in Muskhelishvili (1953), we retrieve the inhomogeneous wave equation

$$S^*_{t^*t^*} - \beta^2 S^*_{x^*x^*} = \mu\alpha^*\sqrt{\frac{1 - x^*}{x^*}}. \tag{24}$$

In contrast to (22), (24) possesses steady solutions that satisfy $S^*(0) = S^*(1) = S^{*\prime\prime}(0)$. If $S^*_{t^*} = 0$ when $t^* = 0$ then β^2 scales with α^* and the steady solution is maintained for all time. If the sail velocity is not initially zero, then once again β changes as the motion progresses.

4.4 *The large tension limit*

For order 1 values of α^* and μ, the possibility arises that the nonlinear length condition (14) might require β to become large for a short period of time during the flow. If this happens, the aerodynamic force will no longer be able to balance the tension force and the dominant balance becomes that between tension and acceleration. In this case, we define a scaled time τ by $\mathrm{d}\tau/\mathrm{d}t^* = \beta$. If we use similar reasoning to that in Section 4.3, the sail equation becomes

$$S^*_{\tau\tau} + \frac{\beta'(t^*)}{\beta^2(t^*)} S^*_\tau = S^*_{x^*x^*} + O(\beta^{-1}). \tag{25}$$

We consider the relative sizes of the terms in (25): if the S^*_τ term dominates, then to leading order $S^*_\tau = 0$ which is plainly absurd. If the term is negligible, then the behaviour of S^* is governed simply by the wave equation with boundary conditions $S^*(0) = S^*(1) = 0$. This leads to oscillatory solutions, contradicting the assumption that β becomes large. It follows that necessarily β'/β^2 is of order 1, in which case $\beta \sim \mid t^* - t_0 \mid^{-1}$ for some t_0.

If large values of β should occur, then we may expect S^* to change rapidly in a short period of time. One possible physical interpretation of this is that the tension becomes so large that the sail breaks. In one case examined numerically below we continued computing even though β became large; however, since the numerical method contains an implicit assumption that the sail does not move by large amounts in any short time period, these results should be treated with suspicion (see Section 7.3).

5. Further properties of the equation of motion

5.1 *Energy*

In order to discuss the energy dissipation of a moving sail it is convenient to rewrite (13) in terms of two variables, yielding

$$S^*_{t^*t^*} - \beta^2 S^*_{x^*x^*} = \mu\gamma^*(x^*, t^*), \tag{26}$$

$$\frac{1}{\pi} \int_0^1 \frac{\gamma^*(\xi^*, t^*)}{\xi^* - x^*} \, \mathrm{d}\xi^* = S^*_{x^*} + S^*_{t^*} - \alpha^*. \tag{27}$$

The first of these equations is essentially Newton's second law, with γ^* representing the aerodynamic force and the $S^*_{x^*x^*}$ term representing the force due to the tension. Since to leading order the applied force is in the y-direction, for a given x^* the distance travelled against the force is given by $\mathrm{d}S^*$ evaluated at fixed x^*, that is, $S^*_{t^*}\mathrm{d}t^*$. This suggests that we may determine the energy by multiplying (26) by S_{t^*} and integrating with respect to x^* between 0 and 1. Performing these computations, we find that

$$\frac{\mathrm{d}}{\mathrm{d}t^*} \left(\tfrac{1}{2} \int_0^1 {S^*_{t^*}}^2 \, \mathrm{d}x^* \right) - \beta^2 \int_0^1 S^*_{t^*} S^*_{x^*x^*} \, \mathrm{d}x^* = \mu \int_0^1 \gamma^* S^*_{t^*} \, \mathrm{d}x^*.$$

The first term in this equation clearly corresponds to the kinetic energy of the sail. The integral in the second term may be integrated by parts to give

$$[S_{t^*} S_{x^*}]_0^1 - \int_0^1 S^*_{x^* t^*} S_{x^*} \, \mathrm{d}x^* = 0 - \frac{\partial}{\partial t^*} \left(\tfrac{1}{2} \int_0^1 {S^*_{x^*}}^2 \, \mathrm{d}x^* \right) = 0,$$

since S_{t^*} is zero at both ends of the sail and the length condition means that the integral over (0, 1) of $S^2_{x^*}$ is constant. Physically, the fact that this integral (being the work done by the tension force on the sail) is zero merely expresses the inability of an inextensible sail to store energy. The energy equation as a whole therefore becomes a balance between the kinetic energy and the energy obtained from the aerodynamic lift. It remains to evaluate the contribution from the latter, which may (if required) be expressed in terms of S^* only using (27). This does not, however, provide a great deal of insight into the problem for order 1 values of μ, and for an inextensible sail it is more convenient to write the energy equation as

$$\frac{\mathrm{d}}{\mathrm{d}t^*} \left(\tfrac{1}{2} \int_0^1 {S^*_{t^*}}^2 \, \mathrm{d}x^* \right) = \mu \int_0^1 \gamma^* S^*_{t^*} \, \mathrm{d}x^*. \tag{28}$$

We see that for $\mu \ll 1$ (a sail of large mass), the energy contribution from the aerodynamic force, which is proportional to μ, is small, and so only the kinetic energy term remains. For small μ therefore, the kinetic energy of the sail is constant and there is no dissipation.

In the case where μ is small but $\alpha^* \mu$ is of order 1, an expression for the energy may again be obtained, since in this case (27) becomes, to leading order,

$$\frac{1}{\pi} \fint_0^1 \frac{\gamma^*(\xi^*, t^*)}{\xi^* - x^*} \, \mathrm{d}\xi^* = -\alpha^*,$$

giving $\gamma^* = \alpha^* \{(1 - x^*)/x^*\}^{\frac{1}{2}}$ (see Muskhelishvili (1953)). Hence the energy equation, from (28), is

$$\frac{\partial}{\partial t^*} \left(\tfrac{1}{2} \int_0^1 {S^*_{t^*}}^2 \, \mathrm{d}x^* \right) = \mu \alpha^* \int_0^1 S^*_{t^*} \sqrt{\frac{1 - x^*}{x^*}} \, \mathrm{d}x^*. \tag{29}$$

This shows that the sail may gain or lose kinetic energy, and in particular that if $S^*_{t^*}$ is of the same sign for all values of x^*, then the sail must gain kinetic energy if this sign is the same as that of α^*, and lose kinetic energy if the signs are opposite. This is the expected result, for a sail moving against the cross-flow is doing work against it and therefore loses energy to it.

5.2 *Stability*

One good reason for proposing and studying the unsteady sail equation (13) is to determine whether or not various steady solutions are stable. It is not immediately clear what is meant by 'stability' in this context, for the length condition (14) ensures that sail deflections

cannot become unbounded. Clearly it is possible, however, for the sail tension (and thus β) to increase even though the length condition is still satisfied. Presumably large sail tensions are likely to appear numerically as increases in β lead to circumstances where it is ever harder for the numerical code to ensure that the length condition is satisfied. We thus interpret 'instability' as exponential growth not in sail deflections, but in β. Other instabilities are also possible; one could imagine, for example, behaviour where the sail develops oscillations whose amplitude tends to zero but whose frequency becomes large (for example, oscillations of the generic type $S(x) \sim \sin(nx)/n$ for large n). We have not observed such behaviour in any numerical experiments.

As far as a complete linear stability analysis is concerned, matters are complicated by the fact that the stability problem does not possess spatially exponential solutions. Linear stability for this problem is currently being investigated, and although some preliminary results have been obtained, discussion of these must be postponed for another study.

6. The numerical scheme

Although it is instructive to analyse asymptotic limits of (13), in general there seems to be no hope of determining closed-form solutions and we are forced to proceed numerically. Since the literature concerning the numerical solution of nonlinear singular partial integro-differential equations seems to be rather sparse (the only previous study that deals with the numerical solution of a related problem seems to be that of Spence & Sharp (1989)), we proceed in an *ad hoc* fashion. Experience has shown that it is almost always a good idea to rearrange singular integral equations so that the highest-order derivatives do not occur under a singular integral operator. We therefore invert (13) according to the methods described in Muskhelishvili (1953) and, for ease of computation, we also set $T = 2t^*$, $X = 2x^* - 1$ and $Y = 2\xi^* - 1$ so that the domain of the problem becomes $(-1, 1)$. The governing equation of motion becomes

$$S^*_{TT} - \beta^2 S^*_{XX} = -\frac{\mu}{2\pi\sqrt{1-X^2}} \int_{-1}^{1} \frac{(S^*_Y + S^*_T)\sqrt{1-Y^2}}{Y-X}\,\mathrm{d}Y + \frac{\alpha\mu}{4}\sqrt{\frac{1-X}{1+X}} + \frac{C(T)}{\sqrt{1-X^2}}. \tag{30}$$

The eigenfunction $C(T)$ must be chosen so that the Kutta condition at $X = 1$ is satisfied, giving

$$C = -\frac{\mu}{2\pi} \int_{-1}^{1} (S^*_Y + S^*_T)\sqrt{\frac{1+Y}{1-Y}}\,\mathrm{d}Y. \tag{31}$$

This equation was solved using an explicit finite-difference formulation in Lattimer (1996). However, this method was limited by the fact that, due to the behaviour of $S^*(X, T)$ near $X = -1$ and the square-root singularities in the formulation (30), accuracy was compromised. An alternative, more accurate numerical formulation may be obtained by using first and second kind Chebyshev polynomials, defined respectively by $T_n(\cos\theta) = \cos(n\theta)$, and $U_n(\cos\theta) = \sin((n+1)\theta)/\sin\theta$ with $\theta = \cos^{-1} X$. The main advantage of using this form of approximation is that, by exploiting some standard properties of

Chebyshev polynomials, all of the required singular integrals may be calculated in closed form, thereby minimizing a substantial source of potential error. To derive a numerical scheme, a number of standard properties of Chebyshev polynomials are required; these are collected together (equations (38)–(49)) for reference in the Appendix.

For the purposes of deriving a numerical scheme, we assume that the solution to (30) may be written as a sum of Chebyshev polynomials in the form

$$S^*(X, T) = \sum_{n=0}^{\infty} a_n(T) T_n(X). \tag{32}$$

On substitution of this expansion into (30) we find that

$$\begin{aligned}\sum_{n=0}^{\infty} \left(\ddot{a}_n T_n - \beta^2 a_n T_n''\right) &= \frac{\alpha\mu}{4}\sqrt{\frac{1-X}{1+X}} \\ &\quad + \frac{\mu}{2\sqrt{1-X^2}} \sum_{n=0}^{\infty} (n a_n T_n - n a_n \\ &\quad + \dot{a}_n[-(1-X^2)U_{n-1} + (X-1)\delta_{n0}])\end{aligned} \tag{33}$$

where derivatives with respect to T and X are denoted using a dot and a dash respectively. By multiplying (33) by T_m and integrating over $(-1, 1)$ we obtain (assuming for the moment that β is known) an infinite system of linear differential equations for the a_n. This system may be written in the form

$$\sum_{n=0}^{\infty} A_{mn}\ddot{a}_n + B_{mn}\dot{a}_n + C_{mn}a_n - \beta^2 D_{mn}a_n = Z_m, \tag{34}$$

where, for $m \geqslant 0$,

$$\begin{aligned}A_{mn} &= -2E_{n+m}\left\{\frac{n^2+m^2-1}{[(n+m)^2-1][(n-m)^2-1]}\right\}, \\ B_{mn} &= \frac{\mu\pi}{8}(\delta_{n,m+1} - \delta_{n,m-1}) - \frac{\mu\pi}{4}\delta_{n0}\delta_{m1} + \frac{\mu\pi}{2}\delta_{n0}\delta_{m0}, \\ C_{mn} &= -\mu n\frac{\pi}{4}(\delta_{nm} + \delta_{n0}\delta_{m0}) + \mu n\frac{\pi}{2}\delta_{m0}, \\ D_{mn} &= nE_{n+m}\left(2n - m\sum_{k=1+(|n-m|/2)}^{k=|n+m|/2}\frac{2}{2k-1}\right), \\ Z_m &= \frac{\alpha\mu\pi}{4}(\delta_{n0} - \delta_{n1}/2).\end{aligned}$$

To form a numerical scheme, we truncate (32) after $N+1$ terms. The linear equations (34) are applied for $0 \leqslant m \leqslant N-2$ and to close the problem and determine the $N+1$ unknowns a_i $(i = 0, 1, \ldots N)$ at a given time we use the boundary conditions $S^*(-1) = S^*(1) = 0$. These give

$$\sum_{n=0}^{N} a_n = \sum_{n=0}^{N} (-1)^n a_n = 0. \tag{35}$$

It is convenient to absorb (35) into our previous definitions by defining the coefficients in (34) for all m and n between 0 and N. This may be accomplished by setting

$$A_{N-1,n} = 1, \quad B_{N-1,n} = C_{N-1,n} = D_{N-1,n} = Z_{N-1} = 0, \quad 0 \leqslant n \leqslant N;$$
$$A_{N,n} = (-1)^n, \quad B_{N,n} = C_{N,n} = D_{N,n} = Z_N = 0, \quad 0 \leqslant n \leqslant N.$$

With these definitions the truncated form of (34) gives sufficient equations to determine the a_n ($0 \leqslant n \leqslant N$) for a given β. To determine β the length condition (14) must be used. From (43) and integration by parts we find that

$$\int_{-1}^{1} S_X^* S_{XT}^* \, \mathrm{d}X = 0 \tag{36}$$

leads, in discretized form, to

$$\sum_{n=0}^{N} \sum_{m=0}^{N} q_{nm} a_n \dot{a}_m = 0,$$

where

$$q_{nm} = nm E_{n+m} \sum_{k=1+(|n-m|/2)}^{k=|n+m|/2} \frac{2}{2k-1}. \tag{37}$$

This implementation of the length condition is tantamount to the assertion that the time derivative of the sail length should be zero. Calculation of the sail length at each instant during the flow therefore provides an additional check that the scheme is performing accurately.

The Chebyshev coefficients a_n and the parameter β may now be determined. We use a finite-difference scheme, employing backward differences for the first derivative. This gives

$$A_{mn} \frac{a_n(T+\Delta T) - 2a_n(T) + a_n(T-\Delta T)}{(\Delta T)^2} + B_{mn} \frac{a_n(T) - a_n(T-\Delta T)}{\Delta T}$$
$$+ C_{mn} a_n(T) - \beta^2(T) D_{mn} a_n(T) = Z_m(T).$$

At each time step, for a given β the new values of a_n may be determined by solving a system of linear equations. This may be accomplished in a very efficient manner, since the coefficient matrix A_{mn} does not vary with time and thus a single LU decomposition may be used throughout. To complete each step a bisection method is used to determine the value of β that causes the length condition to be satisfied.

Numerical experiments using the scheme described above have shown that, as might be expected, for numerical stability the time step ΔT must be chosen to be sufficiently small. Because of the structure of the matrices involved, however, it does not seem easy to determine an analytical expression for a CFL-type condition that would allow the time step to be chosen automatically. Some formal analysis (not given here) has suggested that a suitable stability condition is given by requiring that $n\sqrt{\log n}\beta\Delta T < C$, where C is a constant, and use of this with $C = 0{\cdot}1$ has invariably produced stable results.

TABLE 1
Convergence of mid-sail displacement as N increases ($\lambda = 0{\cdot}5$, $\alpha^* = 1$)

N	10	20	30	40	50	100	200
$S(0{\cdot}5)$	0·59425	0·59262	0·59299	0·59286	0·59293	0·59290	0·59290

7. Results

7.1 *General details and validation*

The scheme described above was coded using FORTRAN. Calculations were carried out using a 200 MHz PC running Linux, the linear equations being solved using the NAG library routines F01BTF and F04AYF. For all of the displayed sail shapes the first 50 or 100 terms of the Chebyshev series were used, though in all cases further runs were carried out to ensure that the results were not unduly sensitive to the value of N used. Some idea of the typical convergence properties of the results as N increases can be gained by studying the dependence of Chebyshev solutions on the steady problem. For example, with $\alpha = 1$ and $\lambda = 0{\cdot}5$, the sail mid-point displacement for various N is shown in Table 1.

The time taken to obtain the numerical solutions varied from case to case, but a few minutes of CPU time may be regarded as a typical run time.

A number of special cases were examined for the purposes of code validation. First, the asymptotic limit $\mu = O(1)$, $\alpha^* \gg 1$ was scrutinized. According to Section 4.2, with $\mu = O(1)$ we should expect to find that, for $\alpha^* \gg 1$, changes in α^* manifest themselves only in changes to β whilst the sail shape is unaltered. In order to test this, computations were begun from the steady solution with $\lambda = 0{\cdot}2$, giving a calculated $\alpha^* = 18{\cdot}257$. The angle of attack α^* was changed according to $\alpha^* = 18{\cdot}257 + t^* (0 \leqslant t^* \leqslant 4)$. The parameter μ was taken to be 1. The results in Fig. 4 show the sail shapes (solid lines) at times $t = 0, 1, 2, 3, 4$; the curves for different times are indistinguishable showing that, in spite of the change in the angle of attack, the sail shape remains virtually unaltered. The symbols show the exact solution to (21), which is given by

$$S^* = \left(\frac{3\pi^2}{128} - \frac{1}{6}\right)^{-1/2} \left[\frac{3\pi x^*}{8} - (x^* - 1/2)\sin^{-1}\sqrt{x^*} - \left(\frac{x^*}{2} + \frac{1}{4}\right)\sqrt{x^*}\sqrt{1 - x^*} - \frac{1}{8}\sin^{-1}(2x^* - 1) - \frac{\pi}{16}\right].$$

The closeness of the agreement suggests that the scheme is performing very satisfactorily for this validation case; a calculation of the ratio β^2/α^* further confirms that, as expected, this quantity is virtually independent of time and takes values within a few per cent of the exact value, which is given by $\mu(3\pi^2/128 - 1/6)^{\frac{1}{2}} \sim 0{\cdot}254$.

In addition to the $\mu = O(1)$, $\alpha \gg 1$ case a number of other validation examples were examined. Space does not permit the inclusion of any details, but our general conclusion was that the code was functioning as expected and was both efficient and reliable.

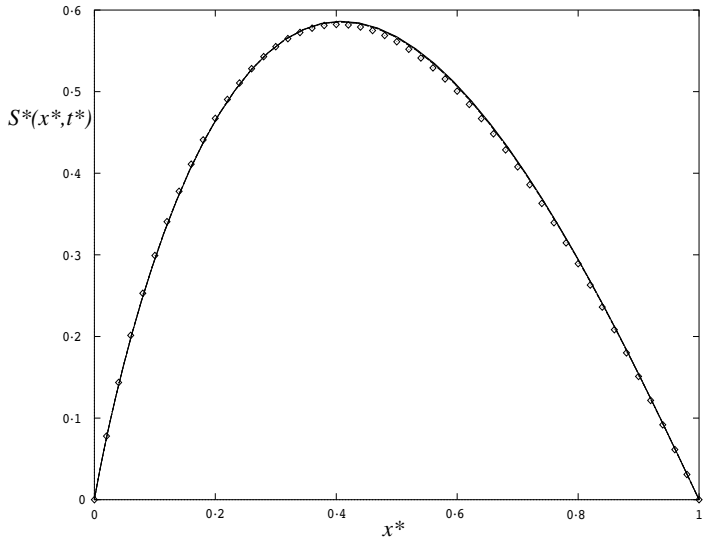

FIG. 4. Validation case with $\alpha \gg 1$, $\mu = 1$. Theoretical sail shape ($\diamond$) and calculated sail shapes for $t^* = 1, 2, 3, 4$ (solid lines; indistinguishable from one another).

7.2 *Changing the curvature of a concave sail*

We now examine a case where we alter the angle of attack α^* so as to change the curvature of a concave sail. We take $\mu = 2$ and start the motion from the steady solution with $\alpha^* = 2$ (so that $\lambda = 1{\cdot}12$ and thus $\beta^2 = \mu/\lambda = 1{\cdot}786$). The value of α^* is then reduced linearly according to

$$\alpha^*(t^*) = \begin{cases} 2 & (t^* \leqslant 0), \\ 2 - t^* & (0 < t^* \leqslant 3/2), \\ 1/2 & (3/2 < t^*). \end{cases}$$

Calculations were performed using Chebyshev series with 100 terms and a time step chosen according to the criterion discussed in Section 6. The general behaviour of the numerical solution is much as one might expect; the sail tension decreases with the angle of attack before oscillating about the steady-state (lowest branch) value corresponding to $\alpha^* = \frac{1}{2}$. The tension parameter β^2 is plotted against non-dimensional time t^* in the top diagram of Fig. 5. Note that when $\alpha^* = \frac{1}{2}$ it is possible for λ to assume a number of different values (see Fig. 2). However, the lowest branch solution corresponding to $\alpha^* = \frac{1}{2}$ has $\lambda = 1{\cdot}854$ and thus $\beta^2 = \mu/\lambda = 1{\cdot}079$; clearly it is this steady-state solution about which the sail oscillates.

The lower plot of Fig. 5 shows the initial steady-state position of the sail ($\diamond$) and the final theoretical steady-state sail shape ($+$). The dashed line shows the sail shape at time $t^* = 16$. It is somewhat unfortunate that solutions on the lower branch of the λ vs. α^* tend

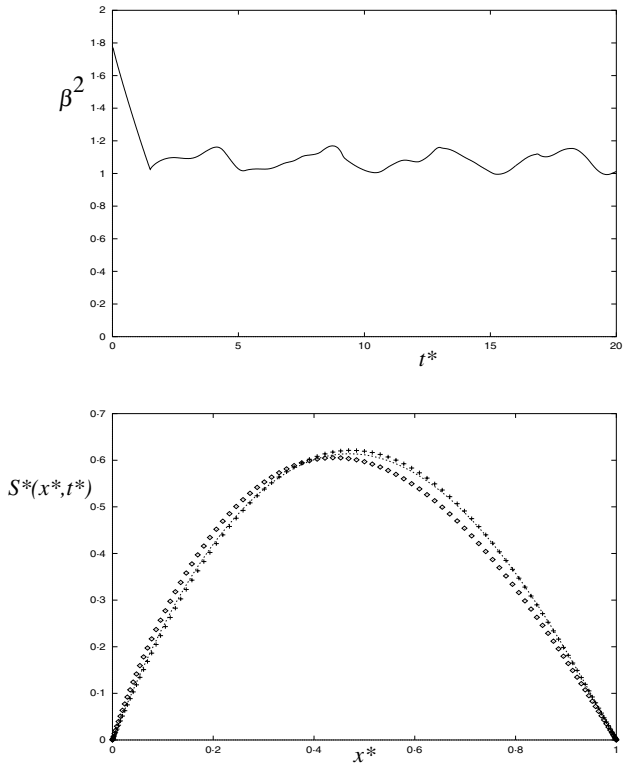

FIG. 5. (Top figure) Tension parameter β^2 vs. t^* as angle of attack α^* changes from 2 to 1/2. (Bottom figure) Original sail shape ($\diamond$), final steady sail shape for $\alpha^* = 1/2$ (+ symbols), calculated sail shape at $t^* = 16$ (dashed line).

to be visually rather similar, and this case is no exception; the similarity between the sail shape for $t^* = 16$ and the 'final' steady-state configuration is nevertheless unmistakable. A careful examination of the kinetic energy and the numerical solution for large t^* shows that the anticipated steady state is reached, albeit rather slowly.

7.3 *A case where the sail tension becomes large*

We shall now examine a case where the tension in the sail becomes large. We take $\mu = 2$, use 100 terms of the Chebyshev series and begin with the steady 'lowest branch' solution corresponding to $\alpha = 1$, giving $\lambda = 1{\cdot}53$ (see Fig. 2). The angle of attack α is now altered; specifically we change α in a linear fashion from $\alpha = 1$ to $\alpha = -1$ over a time interval of length 2. We might expect the sail to change from its initial shape to its mirror image as α changes from 1 to -1. In the first stages of the flow, the successive sail shapes (shown at various times in the bottom part of Fig. 6) suggest that the expected behaviour might materialize: the behaviour of β and the kinetic energy (shown in the top part of Fig. 6) indicates however that the final mirror image state is never approached.

The motion may be analysed using the results. Once the sail begins to move, the tension

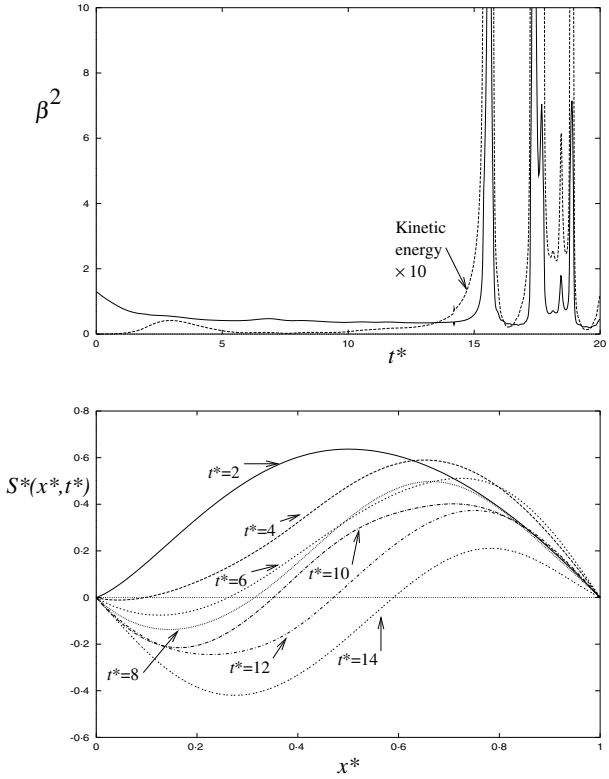

FIG. 6. (Top figure) Tension parameter β^2 (solid line) and $10\times$kinetic energy vs. t^* as angle of attack α^* changes from 1 to -1 for sail with $\mu = 2$. (Bottom figure) calculated sail shapes at various times.

decreases; this decrease is accompanied by downward movement of the front portion of the sail, which continues long after the angle of attack has finished changing. A small rise in the kinetic energy may also be observed. From $t^* = 5$ to about $t^* = 15$, the front part of the sail continues to move further below the axis, but there does not seem to be any approach to a steady state. At about $t^* = 15$ both β^2 and the kinetic energy increase greatly. After this crisis the tension and the kinetic energy briefly recover, but further large increases and decreases are subsequently observed and it seems dangerous to give much credence to the numerical results after $t^* = 15$.

Before $t^* = 15$, it seems that most of the aerodynamic force has gone into accelerating the sail; however, when the sail can no longer accelerate in the negative direction the tension must rise in order to counteract the aerodynamic force. At this point it is clear that the tension term in (30) must be much larger than any other term in the equation, unless S_{tt} is large (the Hilbert transform is bounded everywhere save for $x = 0$ for bounded continuous S_x and S_t). Therefore large values of β may only exist over a time scale of

order β^{-1}, and during this time the sail equation reduces to

$$\frac{1}{\beta^2} S_{tt} - S_{xx} = O(\beta^{-1}).$$

This is the equation obtained in the large mass limit of Section 4.3. Since kinetic energy is conserved by this equation it follows that when β becomes smaller again at the end of this period, the kinetic energy of the sail is still of order β^2. This suggests that S increases for all x, and that the sail shape begins to return above the x-axis. It is only here that the kinetic energy in the sail changes significantly, and there may be several oscillations before the sail changes shape. We conclude that attempting to change the sign of sail curvature is likely to lead to large sail tensions which, as noted above, has implications for the structural integrity of the sail.

The key factor in the occurrence of large values of β is the fact that α changes sign before the sail has moved significantly from its initial profile. This means that the aerodynamic force acts in such as way as to produce negative lift. The resulting negative values of S_t lead to an increase in the kinetic energy of the sail (see (28)). With a sail of smaller mass, however, it is possible for the sail to move significantly before α becomes negative. We therefore conjecture that large values of β may be avoided if a similar experiment is performed on a lighter sail.

7.4 *Motion of a sail of smaller mass*

Since it is evident from the numerical results of Section 7.3 that inertia of the sail is responsible for the high sail tensions that are predicted, we next examine a case where the sail is lighter and so possesses less inertia. When computations are performed for exactly the same case as above in Section 7.3, but with $\mu = 10$, very different behaviour is observed. The tension parameter β^2 and the kinetic energy are shown as functions of time in the top plot of Fig. 7. Once again the motion starts from $\alpha^* = 1, \lambda = 1{\cdot}53$, so that $\beta^2 = \mu/\lambda = 6{\cdot}536$. The tension decreases slowly and then oscillates around a value that may be visually estimated to be about $\beta^2 = 2{\cdot}3$. The top plot of Fig. 7 also shows the kinetic energy (multiplied by a factor of 10). This reaches a maximum soon after the angle of attack has stopped changing, but thereafter remains small. Sail shapes for various times are shown in the bottom plot of Fig. 7; one forms the clear impression that (i) the sail shapes seem to be approaching some sort of steady state and (ii) that steady state is *not* the mirror image of the initial sail shape.

To explain this behaviour it is helpful to re-examine Fig. 2. Presumably any true steady state that the motion eventually assumes or approaches must correspond to a point on the (λ, α^*) curve of Fig. 2. Clearly only one other point on this curve satisfies $| \alpha^* | \simeq 1$, namely the extremity of the next branch up from the bottom one. At this point $\lambda = 4{\cdot}402$. The steady sail shape for this value of λ may be obtained by solving the steady problem in the normal manner; this shape is shown (+ symbols) in the bottom plot of Fig. 7; comparison with the computed sail shapes for later times in the flow provides convincing evidence that the sail is indeed approaching the $\lambda = 4{\cdot}402$ steady shape. We conclude that, for this particular $\alpha^*(t^*)$, instead of reversing the sail has 'jumped a branch' on the (λ, α^*)-diagram.

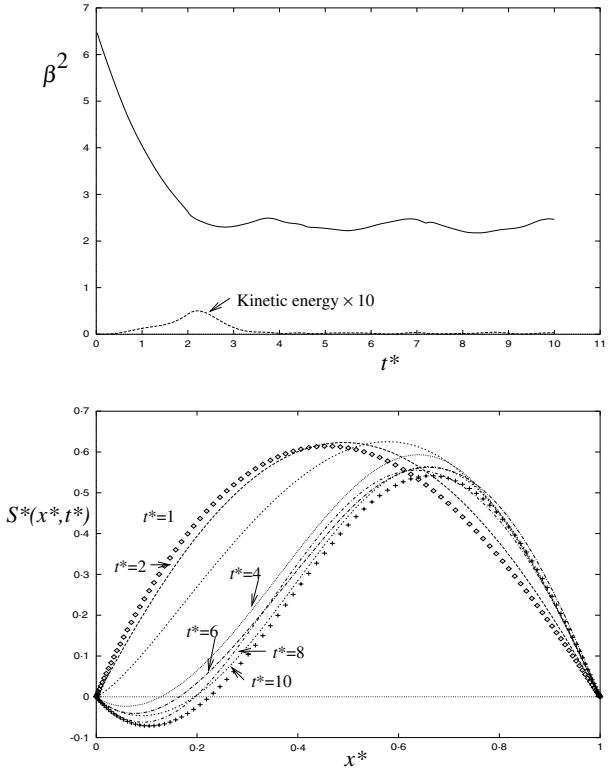

FIG. 7. (Top figure) Tension parameter β^2 (solid line) and 10×kinetic energy vs. t^* as angle of attack α^* changes from 1 to -1 for small mass sail with $\mu = 10$. (Bottom figure) Original sail shape ($\diamond$), final steady sail shape for $\alpha^* = 1$, $\lambda = 4{\cdot}402$ (+ symbols), calculated sail shapes at various times.

One possible explanation for the differences observed between this and the previous test case is that both cases are unstable, but the time at which the instability sets in somehow increases with increasing μ. If this were so, then both this and the last case would be unstable and we simply have not investigated the flow for long enough to observe the instability. Whilst we cannot completely discount this hypothesis, we were unable (with the present parameters) to reproduce the behaviour of the previous example no matter how long we performed calculations for; as time increases the sail simply continues to perform small oscillations about the $\lambda = 4{\cdot}402$ solution. Other similar cases have also been analysed and seem to confirm our present conclusions.

Of course, if the final value of α is so large that only concave sail shapes are possible, then the oscillation observed above around one of the non-concave sail shapes cannot occur. Now the sail must change sign, leading to the sort of instability seen in Section 7.3 whatever the value of μ.

8. Conclusions

A fully unsteady model has been proposed for the motion of a two-dimensional sail in an inviscid, incompressible flow. Although the full model leads to a nonlinear partial singular integro-differential equation to which no closed-form solutions are known, various asymptotic limits may be examined, and in some cases solved. Although some of these limits represent gross simplifications to the full equation, they nevertheless predict behaviour that seems consistent with the physical interpretation of the approximations employed. They also lead, in some instances, to special cases which may be used to validate the numerical method developed for the full equation.

In particular, the analytic solutions found for the light sail (equation (19)) indicate that a non-zero angle of attack can still generate zero lift; a result that mirrors a similar conclusion for the well-studied steady sail case. The problem where the relative angle of incidence is large may also be solved entirely analytically (Section 4.2). In this case the sail shape remains constant and the tension is proportional to the angle of incidence.

Very few previous studies have considered the numerical solution of time-dependent nonlinear integro-differential equations of this sort. This is a little surprising, since such equations inevitably occur when the behaviour of an inviscid main stream is coupled to a perturbation flow. It is worth mentioning that we hope to apply numerical methods similar to this to a variety of other flows as well as to further studies of unsteady sail motion.

As far as numerical results to the full problem are concerned, a variety of different kinds of behaviour have been observed. The results presented in Section 7 show examples of how the shape of the sail, the tension and the kinetic energy vary as the angle of attack changes. In particular we note that for a variation between concave sail shapes with the same sign camber, the sail shape approaches that of the final steady state in a predictable manner, with little oscillatory behaviour. In contrast, when the sail shape changes camber the sail is unable to assume the required final steady-state profile. The tension in the sail becomes large and to all intents and purposes the sail must be deemed to have broken. This difficulty does not occur for lighter sails, which are relatively unaffected by inertia-inducing aerodynamic forces.

A great deal of future work is possible, and some is presently being undertaken. In particular, we are studying the stability of various branches of the steady solution using a standard linear stability method. Another matter that interests us is the elasticity of the sail. If stretching is allowed then it seems that, since sail inertia may be ‘absorbed’ by elastic effects, the problems of high tension in the sail may be largely avoided. Finally, we are considering the behaviour of sails that are not pinned at one end, but which have some bending stiffness. These may be interpreted as ‘stiff flags’, and also have relevance to the air processing of textile sheets and fibres.

Acknowledgement

The second author acknowledges an E.P.S.R.C. studentship, during which most of the research contained in this paper was completed.

References

BÄCKER, M., NEUNZERT, H., & YOUNIS, S. 1991 The fluttering of fibres in air spinning processes.

Proceedings of the Fourth European Conference on Mathematics in Industry (H. Wacker & W. Zulehner eds). Teubner: Stuttgart, pp. 197–205.

BARAKAT, R. 1968 Incompressible flow around porous two-dimensional sails and wings. *J. Math. Phys.* **47**, 327–349.

BUGLER, J. W. 1957 *On the application of potential flow theory to the aerodynamics of sails*, PhD Thesis, College of Aeronautics, Cranfield Institute of Technology.

CHAPLEO, A. Q. 1968 *A review of two-dimensional sails.* Technical report, SUYR report 23, University of Southampton.

CISOTTI, V. 1932 Moto con scia di un profilo flessible. *Accad. Nat. dei Lincei* **15**, 116–173.

DUGAN, J. P. 1970 A free-streamline model of the two-dimensional sail. *J. Fluid Mech.* **42**, 433–446.

HASELGROVE, M. K. & TUCK, E. O. 1976 Stability properties of the two-dimensional sail model. *New England Sailing Yacht Symposium,* Society of Naval Architects and Marine Engineers, pp. 8.1–8.11.

JACKSON, P. S. 1983 A simple model for elastic two-dimensional sails. *AIAA J.* **21**, 153–155.

LATTIMER, T. R. B. 1996 *Singular partial integro-differential equations arising in thin aerofoil theory,* PhD Thesis, University of Southampton.

MUSKHELISHVILI, N. I. 1953 *Singular Integral Equations*. Groningen: Noordhoff.

NICKEL, K. L. E 1987 A theory of sail-wings. *Zeit. Flugwiss. Welt.* **11**, 321–328.

NIELSEN, J. 1963 Theory of flexible aerodynamic surfaces. *J. Appl. Mech. Trans. ASME* **30**, 435–442.

PRANDTL, L. 1918 Tragflügeltheorie I. *Nachr. Ges. Wiss. Goettingen Math. Phys. Kl.* **24**, 451–477.

SMITH, R. & SHYY, W. 1995a Computational model of flexible membrane wings in steady laminar flow. *AIAA J.* **37**, 1769–1777.

SMITH, R. & SHYY, W. 1995b Computation of unsteady laminar flow over a flexible two-dimensional membrane wing. *Phys. Fluids* **7**, 2175–2184.

SPENCE, D. A. & SHARP, P. W. 1989 Distortion and necking of a viscous inclusion in Stokes flow. *Proc. R. Soc.* A **422**, 173–192.

THWAITES, B. 1961 The aerodynamic theory of sails. *Proc. R. Soc.* A **261**, 402–422.

TUCK, E. O. & HASELGROVE, M. 1972 An extension of two-dimensional sail theory. *J. Ship Res.* **16**, 148–152.

VANDEN-BROECK, J. M. 1982 Nonlinear two-dimensional sail theory. *Phys. Fluids* **25**, 420–423.

VAN DYKE, M. 1964 *Perturbation Methods in Fluid Mechanics*. New York: Academic Press.

VOELZ, K. 1950 Profil und auftrieb eines segels. *Zeit. Angew. Math. Mech.* **30**, 301–317.

Appendix: Properties of Chebyshev polynomials

The Chebyshev first and second kind polynomials

$$T_n(x) = \cos(n \cos^{-1} x), \qquad U_n(x) = \sin((n+1)\cos^{-1} x)/\sin(\cos^{-1} x)$$

possess properties that are particularly suited to the development of spectral methods for singular integral equations with Cauchy kernels. The results that are used to derive the numerical scheme discussed in the main text are summarized below. The notation $Q_{nm} = \delta_{n0}\delta_{m0}$ is used, and E_n is defined to be 1 when n is even and 0 otherwise. We also define

$U_{-1}(x) = 0$ for convenience. For integers $m \geqslant 0$ and $n \geqslant 0$ we have

$$\frac{1}{\pi}\fint_{-1}^{1} \frac{U_n(\xi)\sqrt{1-\xi^2}}{\xi - x}\,\mathrm{d}\xi = -T_{n+1}(x), \tag{38}$$

$$\frac{1}{\pi}\fint_{-1}^{1} \frac{T_n(\xi)\sqrt{1-\xi^2}}{\xi - x}\,\mathrm{d}\xi = (1-x^2)U_{n-1}(x) - x\delta_{n0} - \tfrac{1}{2}\delta_{n1}, \tag{39}$$

$$\frac{1}{\pi}\int_{-1}^{1} T_n(\xi)\sqrt{\frac{1+\xi}{1-\xi}}\,\mathrm{d}\xi = \delta_{n0} + \tfrac{1}{2}\delta_{n1}, \tag{40}$$

$$\frac{1}{\pi}\int_{-1}^{1} T_n(\xi)\sqrt{\frac{1-\xi}{1+\xi}}\,\mathrm{d}\xi = \delta_{n0} - \tfrac{1}{2}\delta_{n1}, \tag{41}$$

$$\frac{1}{\pi}\int_{-1}^{1} U_n(\xi)\sqrt{\frac{1+\xi}{1-\xi}}\,\mathrm{d}\xi = 1, \tag{42}$$

$$\int_{-1}^{1} T_m(\xi)U'_{n-1}(\xi)\,\mathrm{d}\xi = E_{n+m}\left(2n - m\sum_{k=1+(|n-m|/2)}^{k=|n+m|/2} \frac{2}{2k-1}\right), \tag{43}$$

$$\frac{1}{\pi}\int_{-1}^{1} \frac{T_n(\xi)T_m(\xi)}{\sqrt{1-\xi^2}}\,\mathrm{d}\xi = \tfrac{1}{2}\left(\delta_{nm} + Q_{nm}\right), \tag{44}$$

$$\frac{1}{\pi}\int_{-1}^{1} T_{m+1}(\xi)U_n(\xi)\sqrt{1-\xi^2}\,\mathrm{d}\xi = \tfrac{1}{4}\left(\delta_{n,m+1} - \delta_{n+1,m}\right), \tag{45}$$

$$\int_{-1}^{1} T_n(\xi)T_m(\xi)\,\mathrm{d}\xi = -2E_{n+m}\left[\frac{n^2+m^2-1}{[(n+m)^2-1][(n-m)^2-1]}\right], \tag{46}$$

$$\frac{1}{\pi}\int_{-1}^{1} \frac{T_n(\xi)}{\sqrt{1-\xi^2}}\,\mathrm{d}\xi = \delta_{n0}, \tag{47}$$

$$\frac{1}{\pi}\int_{-1}^{1} \frac{\xi T_n(\xi)}{\sqrt{1-\xi^2}}\,\mathrm{d}\xi = \frac{\delta_{n1}}{2}, \tag{48}$$

$$T'_n(x) = nU_{n-1}(x). \tag{49}$$